The discrete AlF_5^{2-} fluoroaluminate anion in the structure of $[tetraethylammonium]_2[AlF_5](H_2O)_2$

Gleb Veryasov[a], Kazuhiko Matsumoto*[a], and Rika Hagiwara[a]

Abstract: The first crystallographically defined example of the discrete AlF_5^{2-} fluoroaluminate anion was elucidated via X-ray analysis of $[Et_4N]_2[AlF_5](H_2O)_2$ (Et_4N^+ = tetraethylammonium) single crystals. Intentional preparation of a compound containing the $Al_2F_9^{3-}$ anion via the reaction of two equivalents of $[Et_4N][AlF_4]$ with $[Me_4N]F$ (Me_4N^+ = tetramethylammonium) resulted in the formation of $[Et_4N][Me_4N][AlF_5]$ with unreacted $[Et_4N][AlF_4]$. Cation exchange between these species in the presence of water furnished $[Et_4N]_2[AlF_5](H_2O)_2$ as a precipitate containing the trigonal bipyramidal AlF_5^{2-} anion. The data from the present study allows supplementing the ligand close packing (LCP) model for the 3rd period of the periodic table. The Raman spectrum of $[Et_4N]_2[AlF_5](H_2O)_2$ was analyzed on the basis of quantum chemical calculations.

Introduction

Crystallographic data for the small discrete fluoroaluminate anions continues to be limited due to difficulties related to the growth of single crystals.[1] Following examples of discrete multinuclear complexes of fluoroaluminate anions have been crystallographically characterized in previous studies: $Al_2F_{10}^{4-}$,[2] $Al_2F_{11}^{5-}$,[3] $Al_3F_{16}^{7-}$,[4] $Al_4F_{18}^{6-}$,[3, 5] $Al_4F_{20}^{8-}$,[6] $Al_5F_{26}^{11-}$,[7] $Al_7F_{30}^{9-}$,[8] and $Al_8F_{35}^{11-}$ [3]. Although the chain-type structure of $(Al_2F_9)_n^{3n-}$ is known,[9] the structure of the discrete $Al_2F_9^{3-}$ bioctahedron was first reported in our recent communication in 2013.[10]

In contrast with the diversity of polyfluoroaluminates that have been crystallographically characterized and reported,[11] discrete fluoroaluminate anions, with the exception of AlF_6^{3-} which appears in natural minerals,[12] are poorly investigated. The first report of a fluoroaluminate salt with an organic cation, $[guaH]_3[AlF_6]$ (gua = guanidinium), by Bukovec in 1983[13] inspired other groups for the preparation of isolated hexafluoroaluminates.[14] In 1993 Herron and co-workers reported first discrete tetrahedral units of AlF_4^- appeared in the structure of [1,8-bis(dimethylamino)naphthalene-H]$[AlF_4]$.[15] Single crystals were obtained by the reaction of $[pyH][AlF_4]$ (py = pyridine) with 1,8-bis(dimethylamino)naphthalene in an acetonitrile solution. In another AlF_4^- salts, [collidine-H]$[AlF_4]$ and $[Me_4N][AlF_4]$ (Me_4N^+ = tetramethylammonium), prepared by ion exchange between $[Me_4N]Cl$ and [collidine-H]$[AlF_4]$ (collidine = 2,4,6-trimethylpyridine), a discrete AlF_4^- unit was also determined.[15-16]

The existence of AlF_5^{2-} was originally suggested by Gilbert and his co-workers in 1990[17] based on spectroscopic investigations of NaF–AlF_3 melts. In their further studies, the Al−F stretching band appearing at 555 cm^{-1} in the Raman spectra was considered as a characteristic signal of AlF_5^{2-}.[18] In 1994, Bouyer and his co-workers reported computational modelling of the vibrational spectra of several fluoroaluminates, including AlF_5^{2-}.[19] The obtained spectra appeared to be in good agreement with the experimental results presented by Gilbert,[17] and confirmed the existence of AlF_5^{2-}. Recently, Groß and his co-workers prepared $[Me_4N]_2[AlF_5]$ (Me_4N^+ = tetramethylammonium) by the reaction of $[Me_4N]F$ and $[Me_4N][AlF_4]$; this compound was characterized by Raman spectroscopy and magic angle spinning (MAS) NMR.[1] However, attempts to prepare single crystals of the compound were unsuccessful.

The present study provides the first crystallographic example of AlF_5^{2-} in $[Et_4N]_2[AlF_5](H_2O)_2$ (Et_4N^+ = tetraethylammonium), which has been the matter for discussion for more than 20 years and important insight into the application of the ligand close packing (LCP) model to the third period elements and compounds thereof, including SiF_5^- and PF_5. The LCP model describes molecular geometries based on ligand−ligand repulsions and can provide a more quantitative prediction than the valence shell electron pair repulsion (VSEPR) model, especially for the second period elements[20].

Results and Discussion

In our previous work, we discovered the formation of $[C_{18}C_1im]_3[Al_2F_9](CH_2Cl_2)_{1.754}$ ($C_{18}C_1im^+$ = 1-methyl-3-octadecylimidazolium) containing discrete $Al_2F_9^{3-}$ units, [10] while attempting to crystallize $[C_{18}C_1im][AlF_4]$ from CH_2Cl_2 solution. In the present work, intentional preparation of a compound containing the discrete $Al_2F_9^{3-}$ unit was attempted by the reaction of two equivalents of $[Et_4N][AlF_4]$ with a strong fluoride ion donor $[Me_4N]F$ according to the following route (Eq. (1)):

$$2[Et_4N][AlF_4] + [Me_4N]F \rightarrow [Me_4N][Et_4N]_2[Al_2F_9] \qquad (1)$$

However, the reaction did not produce $Al_2F_9^{3-}$; instead, $[Me_4N][Et_4N][AlF_5]$ was obtained as a precipitate and $[Et_4N][AlF_4]$ remained in the solution; the compositions of both phases were verified by mass balance and Raman spectroscopy (see discussion and Figure S1, ESI) (Eq. (2)):

$$[Et_4N][AlF_4] + [Me_4N]F \rightarrow [Me_4N][Et_4N][AlF_5] \qquad (2)$$

Although the $[Me_4N][Et_4N][AlF_5]$ precipitate was largely insoluble in polar solvents (tetrahydrofuran and acetonitrile), it could be dissolved in dichloromethane. In the presence of water, slow cation exchange between the dissolved $[Me_4N][Et_4N][AlF_5]$ and $[Et_4N][AlF_4]$ occurred, resulting in crystallization of

---

[a] Department of Fundamental Energy Science,Graduate School of Energy Science, Kyoto University, Sakyo-ku, Kyoto 606-8501, JAPAN. e-mail: k-matsumoto@energy.kyoto-u.ac.jp.

Electronic supporting information (ESI) for this article is given via a link at the end of the document.

$[Et_4N]_2[AlF_5](H_2O)_2$ (Eq. (3)):

$$[Me_4N][Et_4N][AlF_5] + [Et_4N][AlF_4] + 2H_2O \rightarrow [Et_4N]_2[AlF_5](H_2O)_2 + [Me_4N][AlF_4] \quad (3)$$

The hydrate, $[Et_4N]_2[AlF_5](H_2O)_2$, was reproducibly obtained from different solvents (CH_2Cl_2/toluene (5/2), CH_3CN, and CH_2Cl_2/THF (10/1) (see ESI for details). All the crystals collected appeared to be suitable for X-ray diffraction; the highest quality crystals, as determined by X-ray diffraction, were grown from the CH_2Cl_2/toluene mixture.

Such reproducibility evidently indicates the high stability of the dihydrate, similar to that observed for the CH_2Cl_2 solvate $[C_{18}C_1im]_3[Al_2F_9](CH_2Cl_2)_n$.[10] The most intriguing fact is that crystals did not form in the absence of water, where water is thought to originate from moisture in the air or in the solvent, indicating that water molecules are essential for stabilization of this lattice. It should be noted that direct crystallization of $[Et_4N][Me_4N][AlF_5]$ from dry dichloromethane gave only powder.

In addition to $[Et_4N]_2[AlF_5](H_2O)_2$, which was obtained as colorless needle-like crystals, a white powder was formed as a by-product after evacuation. Presumably, this precipitate was $[Me_4N][AlF_4]$ that may contain water.

The standard gas-phase enthalpies and Gibbs free energies of AlF_4^-, AlF_5^{2-}, and $Al_2F_9^{3-}$ were calculated at the MP2/aug-cc-pVTZ level and were used to estimate the thermodynamic parameters, ΔH and ΔG, for the following reactions (Eqs. (4) and (5), see Table S1, ESI):

$$AlF_4^- + F^- \rightarrow AlF_5^{2-} \quad (4)$$
$$\Delta H = 248.44\ \mathrm{kJ\ mol^{-1}},\ \Delta G = 286.38\ \mathrm{kJ\ mol^{-1}}$$

$$AlF_4^- + AlF_5^{2-} \rightarrow Al_2F_9^{3-} \quad (5)$$
$$\Delta H = 514.96\ \mathrm{kJ\ mol^{-1}},\ \Delta G = 573.06\ \mathrm{kJ\ mol^{-1}}$$

Although the thermodynamic data indicate that neither process is spontaneous in the gas phase, the second reaction (Eq. 5) is energetically less favorable than the first reaction (Eq. 4). The lattice energy of $[Et_4N][Me_4N][AlF_5]$ is considered to be large because $[Et_4N][Me_4N][AlF_5]$ is a salt of a doubly charged anion, and consequently the reaction summarized in Eq. (4) can proceed in solution. The reaction presented in Eq. (5) is originally not favorable and the high solubility of $[Et_4N][AlF_4]$ prevents the formation of $[Me_4N][Et_4N]_2[Al_2F_9]$.

The hydrate salt, $[Et_4N]_2[AlF_5](H_2O)_2$, crystallizes in the $P4_2/n$ tetragonal space group with a = 24.9774(10) Å and c = 7.1969(4) Å (see X-ray crystallography details, Tables S2 and S3, ESI). Although the crystals obtained were stable in air for a short period (overnight) and did not deliquesce, they may accumulate moisture upon long-term exposure to air, as observed for $[Me_4N]_2[AlF_5]$.[1] Notably, $[Et_4N]_2[AlF_5](H_2O)_2$ had a strong tendency towards twinning. All the crystals checked were twinned with twin fractions ranging from 2 to 50%.

The structure obtained provides the first example of a discrete AlF_5^{2-} anion. Previous attempts to crystallize AlF_5^{2-} salts were unsuccessful due to difficulties in dissolving these salts; Groß and his co-workers reported that $[Me_4N]_2[AlF_5]$ has extremely low solubility in polar solvents.[1] Figure 1 shows the ORTEP diagram of the asymmetric unit of $[Et_4N]_2[AlF_5](H_2O)_2$ determined at −160 °C. The AlF_5^{2-} anion has an AX_5-type trigonal bipyramidal geometry as expected from the VSEPR theory.[21] The Al−F_{eq} (where F_{eq} indicates an equatorial F atom; i.e., F1, F2, and F4 in Figure 1) bonds (1.713(2) − 1.728(2) Å) are shorter than the Al−F_a (F_a indicates an axial F atom; F3 and F5 in Figure 1) bonds (1.768(2) − 1.771(2) Å). The F_a−Al−F_a angle is nearly linear (178.94°) and the F_{eq}−Al−F_{eq} angles (117.0, 127.1, and 115.9°) are close to the ideal angle of 120°. The F_a−Al−F_{eq} angles generated by the axial and equatorial F atoms are close to right angle dimensions (89.0−91.6°). The bond valence sum [22] of the Al atom in AlF_5^{2-} is 3.00 and is consistent with the formal oxidation state of +3 for Al (see Table S4, ESI) for bond valence sum calculations). The contribution from the Al−F_{eq} (average bond valence of 0.630) bond is slightly larger than that of the Al−F_a (average bond valence of 0.553) bond as expected for the trigonal bipyramidal molecules.

The conformation of Et_4N^+ has been discussed in previous studies based on X-ray diffraction and vibrational spectroscopy.[23]

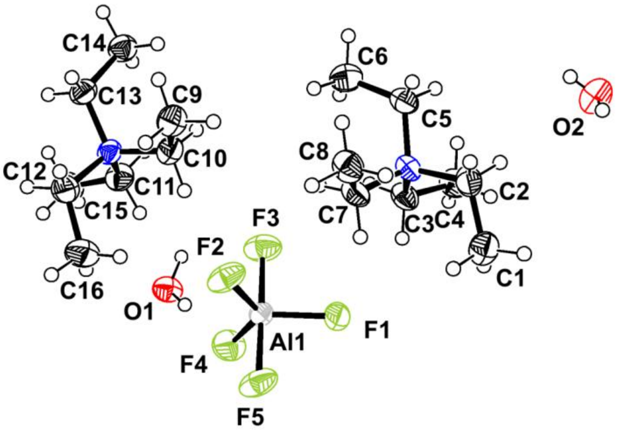

Figure 1. Asymmetric unit of $[Et_4N]_2[AlF_5](H_2O)_2$. Thermal ellipsoids are given at the 50% probability level. Selected bond lengths (Å) and angles (°): Al1—F4 1.713(2), Al1—F2 1.721(2), Al1—F1 1.729(2), Al1—F3 1.768(2), Al1—F5 1.771(2); F4—Al1—F2, 127.08(10), F4—Al1—F1 117.00(10), F2—Al1—F1 115.92(10), F4—Al1—F3 89.39(10), F2—Al1—F3 89.02(10), F1—Al1—F3 91.55(10), F4—Al1—F5 89.83(10), F2—Al1—F5 90.88(10), F1—Al1—F5 89.44(10), F3—Al1—F5 178.94(11).

The Et_4N^+ cations are known to adopt two major conformations; the *TT*-conformation (trans-trans and trans-trans with D_{2d} symmetry) and the *TG*-conformation (trans-gauche and trans-gauche with S_4 symmetry). [23] In the $[Et_4N]_2[AlF_5](H_2O)_2$ structure, both crystallographically independent Et_4N^+ cations adopt the *TT*-conformation.

The molecular packing of $[Et_4N]_2[AlF_5](H_2O)_2$ is shown in Figure 2. The AlF_5^{2-} anions and water molecules form one-dimensional columns along the *c* axis and the Et_4N^+ cations also form a set of one-dimensional columns in the same direction. The distance between two closest axes passing through the Al atoms in the 1D columns is 8.84 Å. The structure is built up by a complicated system of *D*–H···*A* interactions. The *D*–H···*A* interactions in $[Et_4N]_2[AlF_5](H_2O)_2$ are separated into three classes: Et_4N^+–AlF_5^{2-}, AlF_5^{2-}–H_2O, and Et_4N^+–H_2O. The detailed discussion of these interactions is provided in supporting information (see discussion, Tables S5-S7 and Figures S2 and S3, ESI) and is not provided here. In general, water molecules bridge the anions, resulting in the formation of one-dimensional columns running along the *c*-axis, as shown in Figure 2. The O−H···F interactions appeared to be much stronger than C−H···F and C−H···O,

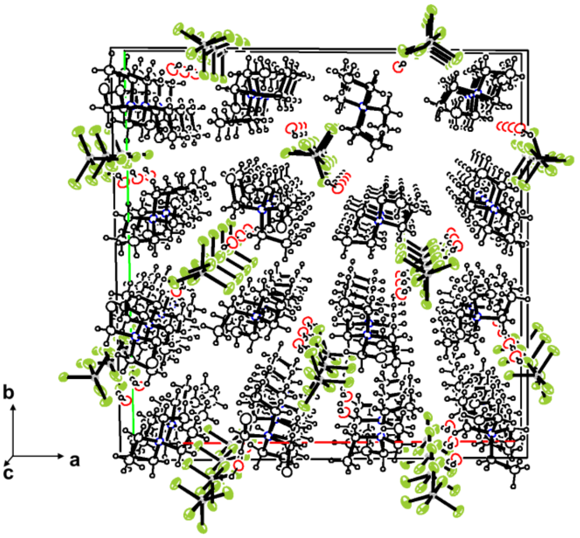

Figure 2. Packing diagram of $[Et_4N]_2[AlF_5]\cdot 2H_2O$ along the *c*-axis. Thermal ellipsoids are given at the 30% probability level (plain ellipsoids are used for clarity).

relevant to Et_4N^+–AlF_5^{2-} and Et_4N^+–H_2O, respectively. Hence, the 1D columns formed by the AlF_5^{2-}–H_2O interactions are essential for stabilization of this crystal lattice.

The Raman spectrum of AlF_5^{2-} has been a matter of discussion[1, 17-18] since the first report of the NaF-AlF_3 molten salt.[17] In the present analysis, the Raman spectrum was recorded for a single crystal that was confirmed as $[Et_4N]_2[AlF_5](H_2O)_2$ by single-crystal X-ray diffraction. The spectra recorded from several different directions suggested that the peak intensities are orientation-dependent. Figure 3 shows the Raman spectrum of the $[Et_4N]_2[AlF_5](H_2O)_2$ single crystal obtained from random direction. The Raman spectrum of $[Et_4N]Cl$ used for identification of the cation bands is presented in Figure S4, ESI; the relative intensities of the bands are listed in Table S6; the spectrum acquired from another direction is shown in Figure S5, ESI. The following assignments are summarized in Table S8 and the bands from cation are listed in Table S9,ESI and based on the calculation at the MP2/aug-cc-pVTZ level (see discussion, Figure S6 and Table S10, ESI).

The most intense band at 558 cm^{-1} is assigned to the $v_s(AlF_{a2})$ + $v_s(AlF_{e3})$ mode. This is the “characteristic” band used by Gilbert and co-workers for identification of AlF_5^{2-}.[18a] The band at 313 cm^{-1} is tentatively assigned as the $\rho_r(AlF_{a2})$ mode given that the $\delta(AlF_{a2})+v_a(AlF_{e3})$ mode is another possible assignment. The two other bands observed at 558 and 628 cm^{-1} are the $v_s(AlF_{a2})+v_s(AlF_{e3})$ and $v_s(AlF_{e3})+\delta(AlF_{a2})$ modes, respectively. The three Raman frequencies observed for $[Et_4N]_2[AlF_5]\cdot 2H_2O$ are in good agreement with those observed for $[Me_4N]_2[AlF_5]$ (322, 563, and 644 cm^{-1}).[1]

Presumably, the contribution of Et_4N^+ and water molecules to the polarizability tensor results in the low intensity of modes A_1' and E' (353 cm^{-1}, 335 cm^{-1}, and 109 cm^{-1} in the calculated frequencies), which precludes their observation in the recorded spectrum. The peaks listed in Table S8 were evaluated from a single random direction; this may account for the discrepancies between the experimental and calculated intensities. The contribution of H···F interactions would affect the frequencies of some vibrational modes, although this remains unaccounted.

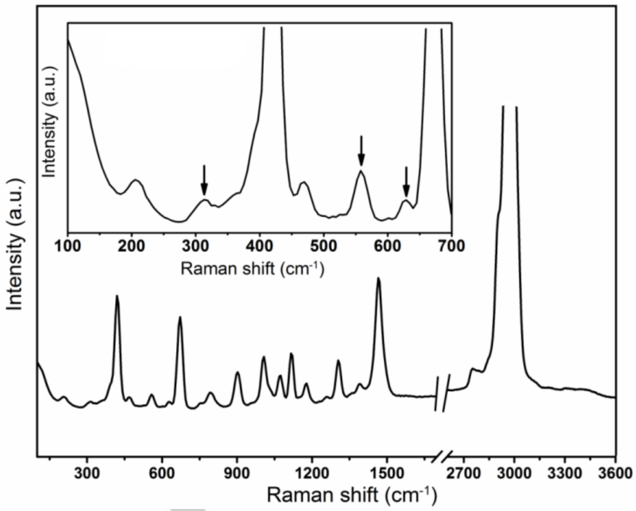

Figure 3. Raman spectrum of $[Et_4N]_2[AlF_5](H_2O)_2$ with enlarged view (inset). The peaks assigned to AlF_5^{2-} are marked with arrows.

The LCP model describes molecular geometries based on ligand−ligand repulsions and can provide a more quantitative prediction than the VSEPR model, especially for the second period elements.[20] Fluorine ligand provides a variety of examples due to its small size and less compressibility. Coordination numbers of only up to four are possible for non-metal period 2 central atoms such as AX_4, and the X···X distances are nearly constant in these molecules.[20] The non-metals of period 3 are large enough to form six-coordinate molecules such as AX_6, as suggested by the LCP model. However, in the case of the four-coordinate AF_4 and five-coordinate AF_5 Si and P complexes, it is clear that the F atoms are not close packed. This can be explained in terms of the large size of the period 3 central atom and the weakness of the A−F bond which cannot bring the four or five F ligands into “contact”.[24] The absence of crystallographic evidence of the trigonal bipyramidal AlF_5^{2-} has hindered discussion of the geometry of fluoroaluminate anions based on the LCP model. The present analysis provides the experimental data for completion of the model. Although the five-coordinate molecules can adopt either trigonal bipyramidal or square pyramidal geometries based on the VSEPR model (and points-on-a-sphere model), the square pyramidal geometry has been observed only in limited cases depending on the compressibility of the ligand.[21b] Herein, AlF_5^{2-} adopts trigonal bipyramidal geometry, where the axial F atom makes contact with the equatorial F atoms but the equatorial F atoms do not make contact with each other. Consequently, the $F_a\cdots F_{eq}$ distance is expected to be twice the radius of the F ligand in this molecule. Table 1 lists the A−F bond lengths and F···F distances in AF_4, AF_5, and AF_6 (A = Al, Si, and P) molecules. In all cases, the F···F distance decreases slightly in moving from AF_6 to AF_5 to maintain close packing of the ligand ($F_a\cdots F_{eq}$ in the case of AF_5) and increases from AF_5 to AF_4, where the F atoms in the AF_4 molecules do not make contact with each other, as mentioned above. The increase in the F···F distance on moving from AlF_5^{2-} to AlF_4^- is more pronounced compared to the other cases. This may be due to the larger size of the Al atom relative to the Si and P atoms, which prevents the F atoms from approaching the Al atom.

Table 1. Average Al−F bond lengths and F···F distances in AF_4, AF_5, and AF_6 (A = Al, Si, and P) molecules.[a]

Anion	A−F, Å	F···F distance, Å
AlF_4^-	1.654 [15]	2.78
AlF_5^{2-}	1.721 (F_e) and 1.770 (F_a)	2.47
AlF_6^{3-}	1.804 [12j]	2.68
SiF_4	1.560 [20]	2.54
SiF_5^-	1.622 (F_e) and 1.660 (F_a) [20]	2.32
SiF_6^{2-}	1.680 [20]	2.38
PF_4^+	1.460 [24]	2.38
PF_5	1.522 (F_e) and 1.585 (F_a) [25]	2.20
PF_6^-	1.580 [21a]	2.24

[a] The F···F distance in AF_5 was calculated as an average of the F_a···F_e distances.

Conclusions

Attempts to prepare an $Al_2F_9^{3-}$ salt via the 2:1 reaction of $[Et_4N][AlF_4]$ and $[Me_4N]F$ resulted in the formation of $[Et_4N][Me_4N][AlF_5]$ and $[Et_4N][AlF_4]$. This mixture yielded $[Et_4N]_2[AlF_5](H_2O)_2$ in the presence of water. The structure of $[Et_4N]_2[AlF_5](H_2O)_2$ is the first crystallographic example of the isolated AlF_5^{2-} with D_{3h} symmetry. The crystallographic data obtained herein was used for completion of the LCP model for discussion of the geometry of 3rd period fluorides (Si, P, and Al). The vibrational spectrum of AlF_5^{2-} anion present in $[Et_4N]_2[AlF_5](H_2O)_2$ was discussed based on the empirical Raman spectra and quantum chemical calculations.

Acknowledgements

This work was financially supported by the Grant-in-Aid for Scientific Research of Japan Society for the Promotion of Science, #26·04763. The advices of Dr. Evgeny Goreshnik (Department of Inorganic Chemistry and Technology, Jožef Stefan Institute, Ljubljana, Slovenia) and Dr. Dmitry Morozov (Department of Chemistry, Nanoscience Center, University of Jyvaskyla, Jyvaskyla, Finland) are gratefully acknowledged.

Supporting information

Experimental details on the synthesis of $[Et_4N]_2[AlF_5](H_2O)_2$, crystallography, ab initio calculations, and Raman spectra measurement. Selected bond lengths for $[Et_4N]_2[AlF_5](H_2O)_2$, bond valence calculations, tables and figures for *D*–H···*A* interactions, geometric parameters for AlF_4^-, AlF_5^{2-}, AlF_6^{3-}, and $Al_2F_9^{3-}$ anions in stationary points, vibrational band assignments for AlF_5^{2-}, geometric parameters for Al, Si and P fluorides. CCDC-1401135 (for $[Et_4N]_2[AlF_5](H_2O)_2$) contain the supplementary crystallographic data for this paper. These data can be obtained free of charge from The Cambridge Crystallographic Data Centre via www.ccdc.cam.ac.uk/data_request/cif.

Keywords: fluoroaluminates • crystallography • Raman spectroscopy • ab initio calculations • LCP model

[1] U. Groß, D. Müller, E. Kemnitz, *Angew. Chem., Int. Ed.* **2003**, *42*, 2626-2629.

[2] F. Kubel, *Z. Anorg. Allg. Chem.* **1998**, *624*, 1481-1486.

[3] K. Adil, M. Leblanc, V. Maisonneuve, *J. Fluorine Chem.* **2009**, *130*, 1099-1105.

[4] a) A. Hemon-Ribaud, M. P. Crosnier-Lopez, J. L. Fourquet, G. Courbion, *J. Fluorine Chem.* **1994**, *68*, 155-163; b) R. B. Ferguson, *Am. Mineral* **1949**, *34*, 383-397.

[5] K. Adil, M. Leblanc, V. Maisonneuve, *J. Fluorine Chem.* **2006**, *127*, 1349-1354.

[6] R. Domesle, R. Hoppe, *Z. Anorg. Allg. Chem.* **1982**, *495*, 27-38.

[7] A. Hemon, A. Le Bail, G. Courbion, *J. Solid State Chem.* **1989**, *81*, 299-304.

[8] E. Goreshnik, M. Leblanc, V. Maisonneuve, *Z. Anorg. Allg. Chem.* **2002**, *628*, 162-166.

[9] A. Le Bail, H. Duroy, J. L. Fourquet, *J. Solid State Chem.* **1992**, *98*, 151-158.

[10] F. Xu, K. Matsumoto, R. Hagiwara, *Dalton Trans.* **2013**, *42*, 1965-1968.

[11] K. Adil, A. Cadiau, A. Hémon-Ribaud, M. Leblanc, V. Maisonneuve, in *Functionalized Inorganic Fluorides*, ed. by A. Tressaud, John Wiley & Sons, Ltd, **2010**, pp. 347-381.

[12] a) L. R. Moras, *J. Inorg. Nucl. Chem.* **1974**, *36*, 3876-3878; b) W. Viebahn, *Z. Anorg. Allg. Chem.* **1971**, *386*, 335-339; c) A. Bystroem, *Ark Kem. Min. Geol.* **1944**, *18*, 10; d) S. Geller, *Am. Mineral.* **1971**, *56*, 18-23; e) G. Cocco, P. C. Castiglione, G. Vagliasindi, *Acta Crystallogr.* **1967**, *23*, 162-166; f) F. C. Hawthorne, R. B. Ferguson, *Can. Mineral.* **1983**, *21*, 561-566; g) A. Hemon, A. L. Bail, G. Courbion, *Eur. J. Solid State Inorg. Chem.* **1990**, *27*, 905-912; h) A. L. Bail, A. Hemon-Ribaud, G. Courbion, *Eur. J. Solid State Inorg. Chem.* **1998**, *35*, 265-272; i) A. Hemon, G. Courbion, *J. Solid State Chem.* **1990**, *84*, 153-164; j) G. Courbion, G. Ferey, *J. Solid State Chem.* **1988**, *76*, 426-431.

[13] P. Bukovec, *Monatsh. Chem.* **1983**, *114*, 277-279.

[14] a) U. Bentrup, M. Feist, E. Kemnitz, *Prog. Solid State Chem.* **1999**, *27*, 75-129; b) U. Calov, R. Seydel, K. H. Jost, R. Hedel, G. Reck, *Z. Anorg. Allg. Chem.* **1993**, *619*, 1939-1944; c) G. Rother, H. Worzala, U. Bentrup, *Z. Anorg. Allg. Chem.* **1996**, *622*, 1991-1996; d) G. Rother, H. Worzala, U. Bentrup, *Z. Kristallogr.-New Cryst. Struct.* **1998**, *213*, 119-120; e) U. Bentrup, A. Ahmadi, H. C. Kang, W. Massa, *Z. Anorg. Allg. Chem.* **1998**, *624*, 1465-1470.

[15] N. Herron, D. L. Thorn, R. L. Harlow, F. Davidson, *J. Am. Chem. Soc.* **1993**, *115*, 3028-3029.

[16] N. Herron, R. L. Harlow, D. L. Thorn, *Inorg. Chem.* **1993**, *32*, 2985-2986.

[17] B. Gilbert, T. Materne, *Appl. Spectrosc.* **1990**, *44*, 299-305.

[18] a) B. Gilbert, E. Robert, E. Tixhon, J. E. Olsen, T. Østvold, *Inorg. Chem.* **1996**, *35*, 4198-4210; b) E. Robert, T. Materne, E. Tixhon, B. Gilbert, *Vib. Spectrosc.* **1993**, *6*, 71-78; c) E. Tixhon, E. Robert, B. Gilbert, *Appl. Spectrosc.* **1994**, *48*, 1477-1482.

[19] F. Bouyer, G. Picard, J.-j. Legendre, *Int. J. Quantum Chem.* **1994**, *52*, 927-934.

[20] R. J. Gillespie, I. Bytheway, E. A. Robinson, *Inorg. Chem.* **1998**, *37*, 2811-2825.

[21] a) R. J. Gillespie, P. L. A. Popelier, *Chemical Bonding and Molecular Geometry*, Oxford University Press, New York, **2001**; b) R. J. Gillespie, I. Hargittai, *The VSEPR Model of Molecular Geometry*, Allyn and Bacon, Boston, MA, **1991**.

[22] I. D. Brown, *J. Solid State Chem.* **1974**, *11*, 214-233.

[23] a) W. A. Henderson, M. Herstedt, V. G. Young, S. Passerini, H. C. De Long, P. C. Trulove, *Inorg. Chem.* **2006**, *45*, 1412-1414; b) C. Naudin, F. Bonhomme, J. L. Bruneel, L. Ducasse, J. Grondin, J. C. Lassègues, L. Servant, *J. Raman Spectrosc.* **2000**, *31*, 979-985; c) H. V. Brand, L. A. Curtiss, L. E. Iton, F. R. Trouw, T. O. Brun, *J. Phys. Chem.* **1994**, *98*, 1293-1301.

[24] E. A. Robinson, R. J. Gillespie, *Inorg. Chem.* **2003**, *42*, 3865-3872.

[25] D. L. Kepert, in *Prog. Inorg. Chem.*, John Wiley & Sons, Inc., **2007**, pp. 41-144.

WILEY-VCH

WILEY-VCH